Adaptive Transparent Force Reflecting Teleoperation with Local Force Compensators

Yushing Cheung and Jae H. Chung
Department of Mechanical Engineering
Stevens Institute of Technology
Castle Point on Hudson
Hoboken, NJ 07030

ABSTRACT- This paper addresses the problems to achieve transparency and contact stability for teleoperation that consists of unconstrained and constrained motions, which are commonly seen in a construction site. The proposed teleoperator used for versatile construction operations keeps human workers from hazardous places. The adaptive bilateral control with a local force compensator is developed based on adaptive impedance control and contact force driven compensation with auto-switching functions. With an unknown slave and construction site dynamics and communication delay, the proposed method guarantees good transparency if no human error exists and low contact force to damp oscillation. Based on an actual haptic device and a virtual manipulator, haptic simulations are presented to demonstrate adaptive transparency and contact stability in the presence of communication delays.

Keywords: teleoperation, robotic intelligence assistance, communication delay, and unstructured environment

1. INTRODUCTION

Due to the increasing number of worksites which are hazardous or inaccessible, remote manipulation, such as space teleoperation, telesurgery, and etc, has become more important and prevalent in recent years. Unfortunately, the unstructured nature of the working environments, especially a construction site, and the limitations of computer decision-making technologies prohibit the use of autonomous systems for remote manipulation. Therefore, it is required that the human decision making be involved in the systems. Teleoperators, in which humans are an integral part of the control, are established to perform the tasks in those environments.

While teleoperation in unstructured sites has been an active topic, two evaluations, transparency and stability have been proposed to assess performance. Handlykken et al.[1] defined transparency as identical positions and forces of master and slave robots. However, even if the transparency can be obtained, the stability is not guaranteed especially during a transition from unconstrained to constrained or vice versa because oscillation excited by contact force at the slave side is difficultly handled by a human operator at the master side. So, a robotic intelligence is needed to assist the human operator based on a local environmental estimation. Among many estimation methodologies, MultInput MultiOutput Recursive Least Square Algorithm (MIMORLS)[2] is the most suitable to be mounted in a PC to compute environment impedances based on more than one inputs, e.g. forces and positions. In addition, a transmission delay between the master and slave is inevitable in practice. The delayed force and visual feedback from the slave can mislead the operator to make an error. The error may cause the teleoperation to be ruined, and the robots, human, environment, or all of them to be damaged. So, the safety of performing teleoperation is required. Nevertheless, a little research has been done for incorporating an error recovering function into the telemanipulator.

Our objective is to develop an adaptive bilateral impedance control method based on the environment estimation (MIMORLS), force compensation, and error recovery switching to ensure stability and transparency. In the proposed method, the master and slave impedances are adapted based on the estimate and their position differences, respectively. If the human error or contact force is detected, the slave robot with the switching and the force compensation assistances can automatically switch to a constrained motion mode to accommodate the force and modify the human commands.

In this paper, we first describe a typical force reflecting teleoperation system. In Sec. 3, the adaptive bilateral control with the force compensator and the auto-switching is proposed. In Sec. 4, two essential performances, transparency and stability, are analyzed in different situations, such as unconstrained, constrained, and transition between them. In Sec. 5, the effect the proposed scheme has on the teleoperation is quantified and qualified by different haptic simulations, and in the last section, the conclusion is drawn based on the simulation results.

2. TELEOPERATION SYSTEM

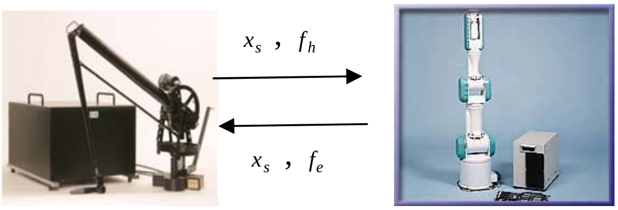

Fig. 1 Haptic Device Fig. 2 Industrial Robotic Arm

Figs. 1 and 2 show the master and slave robots of a typical bilateral teleoperation system, respectively. Each robot is implemented with its local control loops. The other control loops are constructed by establishing communication between the master and the slave. In general, the linearized dynamics of each manipulator is expressed as

Master: $$M_m(\ddot{x}_m-\ddot{x}_s)+B_m(\dot{x}_m-\dot{x}_s)+K_m(x_m-x_s)=C_2\frac{1}{\beta}f_e-f_h \quad (1)$$

Slave: $$M_s(\ddot{x}_s-\ddot{x}_m)+B_s(\dot{x}_s-\dot{x}_m)+K_s(x_s-x_m)=C_3 f_h-\frac{1}{\beta}f_e \quad (2)$$

where x_m and x_s are the n×1 generalized coordinate vectors representing the position and the orientation of the master and slave end effector in their working coordinate systems, respectively, M_m and M_s are the n×n inertia matrices, B_m and B_s are the n×1 vectors representing viscous coefficients of the master and slave robots, respectively, u_m and u_s are the n×1 generalized input vectors for each manipulator, β is the force amplification between the robots, f_h is the n×1 vector representing the operational force vector applied to the human operator by the master manipulator, and f_e is the n×1 vector representing the environmental force sensed by the remote force/torque sensor on the slave arm.

In order to achieve good transparency, i.e. $f_h = f_e$, and $x_m = x_s$ in Eqs. (1) and (2), B_m, B_s, K_m, K_s, C_2, and C_3 are properly selected. However, even if the parameters are well chosen, the perfect transparency can not be obtained because f_h and f_e in Eq. (1) are not equal to those in Eq. (2), respectively in the presence of the communication delay. The system with communication delays will be investigated in Sec. 5.

Besides the issue with transparency, instability is a well-known problem in teleoperation. Until now many stability analyses have been carried out only for constrained or free motion. However, the stability concerning the transition between them has not been fully considered. The major problem in the transition is the oscillation excited by the contact force f_e, which is required to be handled by the telemanipulator and/or the human operator [3, 4]. However, as stated earlier, the oscillation is not easily controlled, especially in the presence of time delay [3].

3. ADAPTIVE BILATERAL CONTROL WITH LOCAL FORCE COMPENSATOR AND AUTO-SWITCHING CAPABILITY

In this paper, the configuration of the teleoperation system as shown in Fig. 3 is used to describe the proposed teleoperation algorithm, and the operator and environment dynamics are assumed to be modeled by a mass-damper-spring system. In Fig. 3, it is assumed that both velocities and forces are subject to communication delay. B_e, K_e are the parameters of the environment, and B_h, K_h, M_h are the parameters of the operator impedance. V_m and V_s are the velocities of the end-points of the master and slave arms. The external forces, F_e^* and F_h^* are independent of the teleoperation system behavior. The contact force switching gain $W(F_e)$ and the force compensator $C_e(F_e)$ at the slave as shown in Fig. 3 are used to switch the mode and minimize the contact force F_e. The master estimator estimates the master impedance based on the contact force and the slave velocity V_s. The slave estimator estimates the slave impedance based on the velocity difference between the slave sensory and the master transmitted readings. Detailed description of the master and slave [2,5] estimators can be found in Secs. 3.1 and 3.2, respectively.

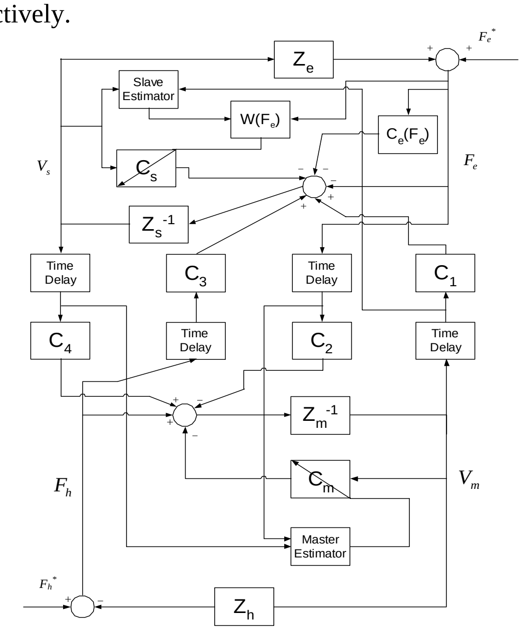

Fig. 3 the proposed bilateral teleoperation system block diagram

Subsystems	Subsystem Dynamics
Master impedance Z_m	$M_m s$
Master controller C_m	B_m+K_m/s
Slave impedance Z_s	$M_s s$
Slave controller C_s	B_s+K_s/s
Velocity channel C_1	B_s+K_s/s
Force channel C_2	$K_f = 1$
Force channel C_3	Not used

Velocity channel C_4	$-(B_m+K_m/s)$
Operator impedance Z_h	$M_h s+B_h+K_h/s$
Task impedance Z_e	B_e+K_e/s
Compliant motion controller $C_e(F_e)$	ν (1/s -1/(s-α)) from Eq. (17)
Switching gain $W(F_e)$	1/(s- ρ) from Eq. (19)

Fig. 4 Nomenclature for the proposed telemanipulation system

3.1 Master Manipulator

In Eqs.(1) and (2), the master damping B_m is adapted to a target damping B_t and M_t equal to M_m, in order to achieve critical damped vibration transmitted to the human operator. The target damping of the compensated robot controller B_t is

$$B_t = 2\varsigma\sqrt{M_t\left(\hat{K}_e + K_m\right)} \quad (3)$$

where B_t is the target damping coefficient, M_t is the target mass, ς is the damping ratio, $\hat{K}_e$ is the estimate of the environment stiffness, and K_m is positive definite in Eq.(1). In the Eq.(3), $\hat{K}_e$, the environment dynamics, can be estimated by the MIMO RLS algorithm proposed by Love and Book et al [2] because the recursive least square estimation is the most suitable for the operator to program in a PC.

3.2 Slave Manipulator

Besides the master adaptation, the slave impedance is also needed to be adapted to achieve a position tracking. Based on the consideration of Lyapunov function of the Eqs.(1) and (2), $V(X,\hat{a}) = X^T PX + \hat{a}^T\Gamma\hat{a}$, and its derivative $\dot{V} = -X^T QX + 2\hat{a}^T vb^T PX + 2\hat{a}^T\Gamma\dot{\hat{a}}$ which can lead to $\dot{V} = -X^T QX$, the adaptation law suggested by Lee, Shin, and Chung et al [5], and Slotine and Li et al [6] is derived as following:

$$\dot{\hat{a}} = -\Gamma vb^T PX \quad (4)$$

where $e = x_s - x'_m$, $X = [e \quad \dot{e}]^T$, Q, P, and A are the symmetric positive definite constant matrices, and for some chosen Q, P satisfies $PA + A^T P = -Q$, $Q = Q^T > 0$, $v = [\ddot{x}'_m - \beta_1\dot{e} - \beta_0 e \quad \dot{x}_s \quad x_s]^T$, $b = [0 \quad 1]^T$, $\hat{a} = [\hat{M}_s \quad \hat{B}_s \quad \hat{K}_s]^T$, and M_s is positive. The convergence of X can be easily shown by Barbalat's lemma [6]. However, even though transparency is obtained, during the transition between constrained and unconstrained motions, the risk of generating large contact force still exists. In the following Eq.(4), the local force compensator $C_e(f_e)$ [7] modified by the contact force f_e is used to model the way in which the natural human muscle changes the stiffness based on the contact force. The local force compensator is:

$$C_e(f_e) = \nu\left[1 - \exp\left(-\alpha\left|f_e\right|\right)\right] \quad (5)$$

where f_e is the contact force, ν is a positive constant, and α is $\alpha[k+1] = \alpha[k] + l(f_e[k] - f_e[k-1])f_e[k]$ where $\alpha[n]$ is the variable at time = n, l is a positive constant, and $f_e[n]$ is the contact force at time = n. As mentioned earlier, controlling a master-slave manipulator has been a challenging problem when the system has to cope with two opposite situations, unconstrained and constrained motions [8]. The reason is the position and force controls are differently required in either of the motions. In addition, the human error may exist during teleoperation. Therefore, the switching capability is required to allow the system to change its mode in the different situations. Moreover, the system is not supposed to be switched to the situation where the local force compensator is not large enough to accommodate the force. Hence, by choosing ρ = α in Eq. (6), the contact force based switching gain $W(f_e)$ takes the same form of the exponential function in Eq. (5). The switching gain is decreased or increased at the same speed that the compensator is increased or decreased, respectively. So, the switching gain is proposed as

$$W(f_e) = \exp\left(-\rho\left|f_e\right|\right) \quad (6)$$

where ρ is a positive constant.

By incorporating Eqs.(3),(4),(5),and (6), the resulting dynamic equations of the teleoperator in Fig. 3 is proposed as

Master $\quad M_m\ddot{x}_m + \left(B_m + \hat{B}_m\right)\left(\dot{x}_m - \dot{x}'_s\right) + K_m\left(x_m - x'_s\right) = u'_m \quad (7)$

Slave $\quad M_s\left(\ddot{e} + \beta_1\dot{e} + \beta_0 e\right) = -f_e C_e\left(f_e\right) + V^T\tilde{a} \quad (8)$

where $V = [z \quad \dot{x}_s \quad x_s]^T$,
$\tilde{a} = \left[W(f_e)\hat{M}_s - M_s \quad W(f_e)\hat{B}_s - B_s \quad W(f_e)\hat{K}_s - K_s\right]^T$, and
$u'_m = f'_e - f_h$

4. TWO ESSENTIAL EVALUATIONS: TRANSPARENCY AND STABILITY

The proposed telemanipulation system is evaluated in terms of transparency and stability. Until now many teleoperation stability problems have been analyzed by the passivity theory. However, it is too conservative [9], especially for the transition between unconstrained and constrained motions. Therefore, the Lyapunov method is adopted here instead. Three situations, unconstrained, constrained motion, and transition between them, are considered to investigate the performance of the developed method.

4.1 Unconstrained Motion Mode

4.1.1 Transparency

Due to no contact force f_e, $W(f_e)=1$ in Eq. (8). Then, the system is switched to the unconstrained motion mode. In order to achieve the transparency during the unconstrained motion, the slave position x_s should closely track the master position x_m. By the adaptation law in Eq. (14), as long as the estimates of the impedance parameters $\hat{M}_s, \hat{B}_s, \hat{K}_s$ approach certain values, the position error e is to become zero, which will cause $x_s = x'_m$. Therefore, the transparency can be enhanced.

4.1.2 Stability

Within the unconstrained space, the local force compensator $C_e(f_e)$ in Eq. (8) becomes meaningless due to no contact force. A Lyapunov candidate $V_u(X_u)$ is the total energy of the system, which consists of the total kinetic energy and total potential energy as

$$V_u(X_u)=\frac{1}{2}\left(M_m\dot{x}_m{}^2+K_m(x_m-x'_s)^2\right)+\frac{1}{2}\left(M_h\dot{x}_m{}^2+K_h(x_d-x_m)^2\right) + \frac{1}{2}M_s\dot{x}_s{}^2+\frac{1}{2}M_s\beta_0(x'_m-x_s)^2 \tag{9}$$

where $X_u=[x_m-x'_s \quad x'_m-x_s \quad x_d-x_m \quad \dot{x}_s \quad \dot{x}_m]^T$, and the equilibrium point is X_u = 0. Then, the Lyapunov function $V_u(X_u)$ can be shown to be positive definite as following:

$$\dot{V}_u(X_u)=-B_m(\dot{x}'_s-\dot{x}'_m)^2-M_s\beta_1(\dot{x}_s-\dot{x}'_m)^2-B_h\dot{x}_m{}^2 \tag{10}$$

Then, $V_u(X_u)$ tends to infinity as X_u tends to infinity, and $\dot{V}_u(X_u)\le 0$ over the whole state space. Thus, the states of the system asymptotically converge to the equilibrium point. Furthermore, according to the environment stiffness estimate, $B_m=B_t$ is decreased. Therefore, the operator's effort can be relieved.

4.2 Constrained Motion Mode

4.2.1 Transparency

During the contact with the environment, the contact force f_e is increased and therefore, $W(f_e)$ is decreased to 0 in Eq. (8). Therefore, the local force compensator $C_e(f_e)$ in Eq. (8) is initiated to accommodate the increased contact force. Hence, as the contact force f_e becomes very large, the slave end-effector position is maintained at the equilibrium position x_0 regardless of the value of the transmitted master position x_m. Then, the oscillation excited by the large contact force can be avoided on account of the human error, the temporary communication blackout between two robots, or etc.

4.2.2 Stability

On the other hand, in the constrained motion, a Lyapunov candidate $V_c(X_c)$ can be written as

$$V_c(X_c)=\frac{1}{2}\left(M_m\dot{x}_m{}^2+K_m(x_m-x'_s)^2\right)+\frac{1}{2}\left(M_h\dot{x}_m{}^2+K_h(x_d-x_m)^2\right)+\frac{1}{2}M_s\dot{x}_s{}^2 +\frac{1}{2}C_e(f_e)K_e(x_s-x_o) \tag{11}$$

where $X_c=[\Delta x'_m-\Delta x_s \quad \Delta x_m-\Delta x'_s \quad \dot{x}_m \quad \dot{x}_s \quad \Delta x_m \quad \Delta x_s]^T$, $\Delta x_m=x_m-x_{m1}$, $\Delta x_s=x_s-x_{s1}$, $\Delta x'_m=x'_m-x'_{m1}$, $\Delta x'_s=x'_s-x'_{s1}$, x_{m1} and x_{s1} are two constants satisfying $x_d\ge x_{m1}\ge x_{s1}\ge x_o$, x'_{m1} and x'_{s1} are two constants satisfying $x_d\ge x'_{m1}\ge x'_{s1}\ge x_o$, and the equilibrium point is X_c = 0. Then, the Lyapunov function $V_u(X_u)$ can be shown to be positive definite as following:

$$\dot{V}_u(X_u)=-B_m(\dot{x}_m-\dot{x}_s)^2-B_s(\dot{x}'_m-\dot{x}_s)^2-B_h\dot{x}_m{}^2-C_e(f_e)B_e\dot{x}_s \tag{12}$$

Then, $V_c(X_c)$ tends to infinity as X_c tends to infinity, and $\dot{V}_c(X_c)\le 0$ over the whole state space. So the states of the system asymptotically converge to equilibrium point. Therefore, based on the contact force f_e and the estimate of the environment, the increased local force compensator $C_e(f_e)$ and $B_m=B_t$ can enhance the stability of the system during the contact.

4.3 Transition Mode

4.3.1 Transparency

After a finite number of switchings between the unconstrained ($W(f_e)$=0) and constrained ($W(f_e)$=1) motions, the system will remain in the constrained space and converge to the equilibrium position x_{eq} asymptotically where $x_m\ge x_{eq}\ge x_o$. As mentioned above, in case the contact force f_e is increased or decreased, x_{eq} tends to x_o or x_m, respectively. So, it can automatically correct the faculty position commands given by the human or whatever may cause unstable oscillation. After a corrective action is taken, the transparency will be enhanced according to the adaptation law in Eq. (4).

4.3.2 Stability

According to Eqs. (10) and (12), the derivatives of the Lyapunov functions in unconstrained and constrained spaces are not equal i.e. $\dot{V}_u(X_u)\ne\dot{V}_c(X_c)$. A uniform Lyapunov function of the switching system cannot be defined. However, we can still prove the asymptotic stability from the energy point of view.

It has previously been proved that within the unconstrained or constrained space, the derivatives of the Lyapunov function $\dot{V}$ are less than or equal to 0. Therefore, between two adjacent switching instances, there is a non-zero decrease in V as long as $V \geq P_0$ where $P_0 = \frac{1}{2}K_m(x_s' - x_m)^2 + \frac{1}{2}K_h(x_d - x_m)^2 + \frac{1}{2}C_e(f_e)K_e(x_s - x_o)^2$. Then there must exist a switching instance t_{2k}, such that $V > C$ at t_{2k}, but $V \leq C$ at t_{2k+2}. Ni and Wang et al [10] found out that the teleoperator could not leave the constrained space when $V \leq C$ where in this paper, C is equal to $\frac{1}{2}C_e(f_e)K_e(x_0 - x_s)^2 + P_0$. Hence, the system will approach the equilibrium position. The overall stability is achieved. The performance improvement will be quantified by haptic simulations, and the simulation results will be discussed in the next section.

5. HAPTIC SIMULATION RESULTS

x_m , f_h $\rightarrow$

x_s , f_e $\leftarrow$

Fig. 5 Haptic Device Fig. 6 Virtual Robotic Arm

The four haptic simulations performed were the human operation controlled haptic device shown in Fig. 5 to manipulate the virtual slave robotic tip positions shown in Fig. 6 with different control methods. The prescribed task was the slave robot end-effector moved from the home position to the right wall. After the contact was made, the end-effector moved towards front and then back to the home position. During the contact, the operator tried to maintain contact pressure against the wall but failed due to the predefined contact 100 (msec) transmission delay. The delay was chosen in the simulations because there is the critical value beyond which the system will be unstable [11].

It was assumed that during the simulations, no friction occurred between the end-effector and virtual wall, no gravity existed, the masses were constant, and air resistance was negligible. Only the direction perpendicular to the wall was considered in the simulations. The normal displacement from the home position to the virtual wall mapped into the master workspace was 0.8 m. As shown in Figs. 7 – 14, the master force was the amount of force that was felt by the human through the haptic device. The slave force was the amount of force that was computed by solving the environment dynamic equation with the above parameters and scaled down by 10. If the maximum scaled down slave position and force were larger than 0.9 m and 6 N, respectively, the environment was damaged. The following parameters were used. M_s = 30 kg, B_s = 1.0 Ns/m, M_m = 0.22 kg, B_m =0.01 Ns/m, B_e = 0 Ns/m, K_e = K = 60 N/m, β_0 = 10000, β_1 = 200, $\varsigma = 1$, β = 10, K_m =10 N/m, Γ = diag(0.001, 63, 50000), , t_d = 0.1 seconds, l =0.5, ρ =1.5, ν = 0.667, and $\alpha[0] = 1.5$

Simulation 1 Robust Control

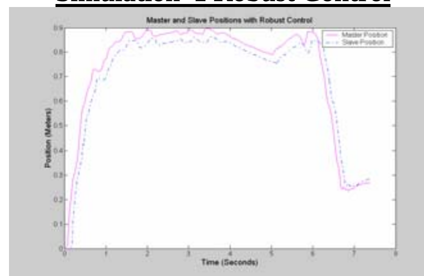

Fig. 7 Master and Slave Positions

Fig. 8 Master and Slave Forces

Simulation2 Adaptive Impedance Control

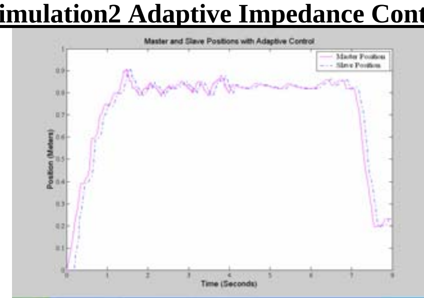

Fig. 9 Master and Slave Positions

Fig. 10 Master and Slave Forces

Simulation 3 Robust Control with Local Force Compensator

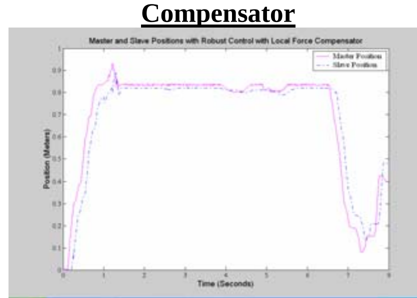

Fig. 11 Master and Slave Positions

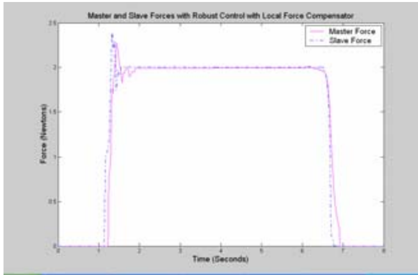

Fig. 12 Master and Slave Forces

<u>Simulation 4 Adaptive Impedance Control with Local Force Compensator</u>

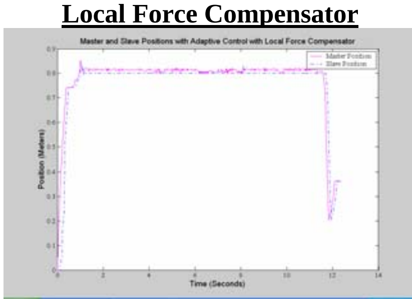

Fig. 13 Master and Slave Positions

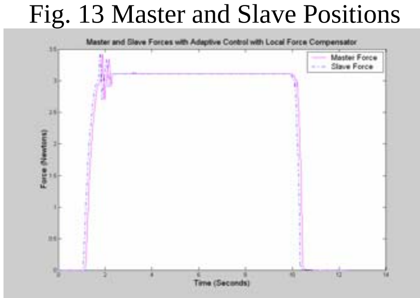

Fig. 14 Master and Slave Forces

By comparing the above results using different types of controllers, the position tracking and the vibration reduction were the worst in the teleoperation without robotic intelligence assistance, such as simulation 1. With the intelligence assistance, such as simulation 2, 3 and 4, the system can perform better position tracking and vibration reduction.

6. CONCLUSION

It was demonstrated through haptic simulations that the developed adaptive impedance control method with local force compensators was an effective solution to the problem of minimizing the oscillation caused by the large contact force in the constrained motion and improving the transparency of the teleoperation in the free motion. In addition, the developed system replaces the manual switching function with an intelligent scheme and avoids large contact forces due to the human error. The system inherits the cited benefits from the characteristics of the local force compensator, the adaptive impedance control, and the force based switching function.

REFERENCES

[1] M. Handkykken and T. Turner, “Control System Analysis and Synthesis for a Six Degree-of-freedom Universal force-reflecting Hand Controller”, *Proc. IEEE Conf. Decision and Control*, 1980

[2] L.J. Love and W.J. Book, “Force reflecting teleoperation with adaptive impedance control”, *Systems, Man and Cybernetics, Part B*, IEEE Transactions on Volume 34, Issue 1, Feb. 2004 Page(s):159 – 165

[3] B. Hannaford and R. Anderson, “Experimental and Simulation Studies of Hard Contact in Force Reflecting Teleoperation”, *Proc. IEEE Int. Conf. Rob. & Auto.*, pp. 584-589, 1988.

[4] T. Chan, S. Everett, and S. Dubey, “Variable damping impedance control of a bilateral telerobotic system”, *Proc. Int. Conf. Robotics Auto.*, 1996, pp. 2033-2040

[5] H.K. Lee, M.H. Shin, and M.J. Chung, “Adaptive Controller of Master-Slave Systems for Transparent Teleoperation”, *ICAR ’97*, Monterey, CA, July 7-9, 1997

[6] J.J.E. Slotine and W. Li., “On the Adaptive Control of Robot Manipulators”, *Int. Journal Robotics Release*, Vol. 6, No.3, pp. 49-59, 1987.

[7] O.M. Al-Jarrah and Y.F. Zheng, “Intelligent Compliant Motion Control”, *Pro. of 1996 IEEE Int. Conf. on Robotics and Automation Minneapolis*, Minnesota-April 1996

[8] A. Rubio, A. Avello, and J. Florez, “Adaptive impedance modification of a master-slave manipulator”, *Robotics and Automation, 1999.* IEEE International Conference on Volume 3, 10-15 May 1999 Page(s):1794 - 1799 vol.3

[9] J.H. Ryu, D.S. Kwon, and B. Hannaford, “Stable teleoperation with time-domain passivity control”, *Robotics and Automation*, IEEE Transactions on Volume 20, Issue 2, April 2004 Page(s):365 - 373 Digital Object Identifier 0.1109/TRA.2004.824689

[10] L. Ni and D.W.L. Wang, “Contact transition stability analysis for a bilateral teleoperation system”, *Robotics and Automation 2002. Proceedings*, ICRA '02. IEEE International conference on Volume 3, 11-15 May 2002 Page(s):3272 – 3277 Digital Object Identifier 10.1109/ROBOT.2002.1013731

[11] S. Suomela and A. Halme, “Tele-existence Techniques of Heavy Work Vehicles”, *Autonomous Robots*, Vol. 11, No. 1 July 2001